Author(s): Larciprete, M. C. & Albertoni, A. & Belardini, A. & Leahu, G. & Li Voti, R. & Mura, F. & Sibilia, C. & Nefedov, I. & Anoshkin, I. V. & Kauppinen, Esko I. & Nasibulin, Albert G.

Title: Infrared properties of randomly oriented silver nanowires

Year: 2012

Version: Final published version

Please cite the original version:

Larciprete, M. C. & Albertoni, A. & Belardini, A. & Leahu, G. & Li Voti, R. & Mura, F. & Sibilia, C. & Nefedov, I. & Anoshkin, I. V. & Kauppinen, Esko I. & Nasibulin, Albert G. 2012. Infrared properties of randomly oriented silver nanowires. Journal of Applied Physics. Volume 112, Issue 8. 083503/1-6. ISSN 0021-8979 (printed). DOI: 10.1063/1.4759374

Infrared properties of randomly oriented silver nanowires

M. C. Larciprete, A. Albertoni, A. Belardini, G. Leahu, R. Li Voti, F. Mura, C. Sibilia, I. Nefedov, I. V. Anoshkin, E. I. Kauppinen, and A. G. Nasibulin

Citation: Journal of Applied Physics **112**, 083503 (2012); doi: 10.1063/1.4759374
View online: http://dx.doi.org/10.1063/1.4759374
View Table of Contents: http://scitation.aip.org/content/aip/journal/jap/112/8?ver=pdfcov
Published by the AIP Publishing

Infrared properties of randomly oriented silver nanowires

M. C. Larciprete,[1,a)] A. Albertoni,[2] A. Belardini,[1] G. Leahu,[1] R. Li Voti,[1] F. Mura,[1] C. Sibilia,[1] I. Nefedov,[3] I. V. Anoshkin,[4] E. I. Kauppinen,[4] and A. G. Nasibulin[4]
[1]*Dipartimento di Scienze di Base ed Applicate per l'Ingegneria, Sapienza Università di Roma, Via A. Scarpa 16, 00161 Roma, Italy*
[2]*IR Detection Division, BFi OPTiLAS Italy, Via E. De Marchi 27, 00144, Roma, Italy*
[3]*School of Electrical Engineering SMARAD Center of Excellence, Aalto University, P.O. Box 13000, 00076 Aalto, Finland*
[4]*Department of Applied Physics, Aalto University School of Science, P.O. Box 15100, Puumiehenkuja 2, Espoo 00076, Finland*

(Received 18 April 2012; accepted 25 September 2012; published online 16 October 2012)

We experimentally investigated the infrared properties of a set of randomly oriented silver nanowires films deposited onto glass substrate. Infrared emission of the obtained films was characterized in the long infrared range, i.e., 8–12 μm, by observing their temperature evolution under heating regime with a focal plane array infrared camera as well as a thermocouple. The obtained experimental results showed that the infrared emission from a mesh composed of silver nanowires might be tailored by opportunely assessing preparation condition, such as the metal filling factor. From the theoretical point of view, the real and imaginary part of the electrical permittivity components were retrieved from the calculations of effective permittivities of in-plane randomly oriented metallic wires, thus giving the refractive index and extinction coefficients for the four different silver nanowires meshes. Due to the correspondence between emissivity and absorbance, the experimental results are interpreted with the reconstructed corresponding absorbance spectra, thus suggesting that these coatings are suitable for infrared signature reduction applications. © *2012 American Institute of Physics*. [http://dx.doi.org/10.1063/1.4759374]

I. INTRODUCTION

In the seek of the perfect absorber[1] and selective emitter,[2–6] several proposals have been developed and demonstrated at infrared (IR) frequencies, for sensing, thermophotovoltaics, and security applications. This is witnessed by the increasing interest in developing wavelength selective IR devices exploiting their photonic,[7–9] phononic,[10] and plasmonic[11–14] properties.

Considering IR radiation, the term *infrared signature* generically describes how objects appear to infrared sensors. The infrared signature of a given object depends on several factors, including the shape and size of the object, its temperature and its emissivity, as well as external conditions (i.e., illumination, surface, environment, etc.). One of the most challenging tasks is to reduce the infrared signature of an object at a given temperature. By definition, the IR spectrum is very wide, spanning the range from 0.77 to 1000 μm, i.e., from the red-light to microwave radiation. However, only two atmospheric windows pertain high IR transmittance, i.e., 3–5 and 8–12 μm, known as mid wavelength IR (MWIR) and long wavelength IR (LWIR) windows, respectively. Outside these windows, attenuation of IR radiation is strong, due to the role of CO_2 and H_2O vapour in both absorption and scattering phenomena.[15]

The idea behind selective thermal emission relies on the control of material spectral absorbance which is equivalent to managing material emissivity. Although several works have been made within this frame, as already mentioned, very few relies on randomly oriented structures, i.e., configurations that avoid complicated preparation steps and high costs.

Very recently, subwavelength structures composed of metallic nanowires have been realized[16–20] and successfully employed for the realization of several nanoelectronics devices. By definition, nanowires have cross-sectional dimensions that can range between 2 and 200 nm, while their lengths span from hundreds of nanometres to some millimetres. Nanowires based metamaterials have been designed, where metallic nanowires are opportunely arranged into a dielectric matrix.[21] In Ref. 21, an array of parallel silver nanowires was opportunely arranged into a porous alumina matrix, with their axis perpendicularly oriented with respect to the matrix surface and it was shown that when the separation distance between the nanowires is smaller than the incidence wavelength, these structures behave as a so-called "indefinite material," i.e., a medium where the two dielectric constants, parallel and perpendicular to the nanowires, respectively, have opposite sign.[21–23] In addition, metallic nanowires show peculiar optical properties, such as high optical transmittance in the visible range, connected to the extremely reduced dimension of wires diameter, while still allowing for good electrical conduction,[24] thus being suitable for manipulation of IR radiation.

In the present work, we aim to exploit the selective emitting properties of films composed of silver nanowires, randomly oriented in the horizontal plane and deposited onto glass substrate, for IR signature reduction. The structures were characterized through emissivity measurements using a

[a)]Author to whom correspondence should be addressed. Electronic mail: mariacristina.larciprete@uniroma1.it.

TABLE I. Geometrical parameters and filling factor of the investigated Ag-nanowires films.

	Diameter [nm]	Length [μm]	Solution concentration [% wt]	Filling factor
NW1	100	20–50	0.005	0.05
NW2	100	20–50	0.01	0.14
NW3	60	5–15	0.005	0.08
NW4	60	5–15	0.01	0.20

focal plane array (FPA) infrared camera operating in the long wavelength infrared range, i.e., 8–12 μm, showing the tuning of infrared emission with different metal filling factors.

II. INFRARED THERMOGRAPHY CHARACTERIZATION

For sample preparation, we utilised two different suspensions of Ag-nanowires in isopropanol (IPA) (starting concentration 5% wt), purchased from Seashell Technology. For both short and long nanowires, two solutions were prepared, using 0.1 ml of the IPA dispersion and an amount of de-ionized water (either 50 or 100 ml, respectively). The geometrical parameters of the nanowires, as well as details of the obtained solutions in water, are presented in Table I. The Ag-nanowires in suspensions were ultrasonicated, filtrated, and transferred onto a glass substrate, following a procedure similar to that described in Refs. 25 and 26, giving a film which is schematically illustrated in Figure 1. In Figure 2, we show the scanning electron micrograph (SEM) images obtained for fabricated films, where blue frame holds for

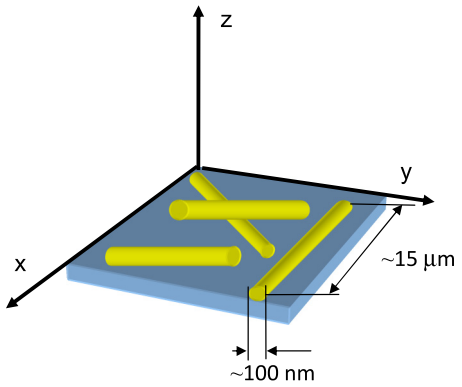

FIG. 1. Schematic drawing of the proposed nanowires based infrared absorber.

long type nanowires (a) low density and (b) high density, and red frame holds for short type nanowires (c) low and (d) high density, respectively. In order to compare the different nanowires density, same magnification was employed for all samples.

Quantitative characterization of infrared radiation, also known as infrared thermography, is retrieved from the infrared images obtained using a calibrated IR-camera (i.e., radiometric camera). The infrared emission of the Ag-nanowires coatings was thus measured and compared to the emission of the bare heating source. Samples were placed onto a hotplate holder, acting as the heat source, allowing maximum heating temperature +200 °C with fast heating-up by powerful integrated electrical heater, homogenous temperature distribution, and over-temperature protection inside the plate. A clear

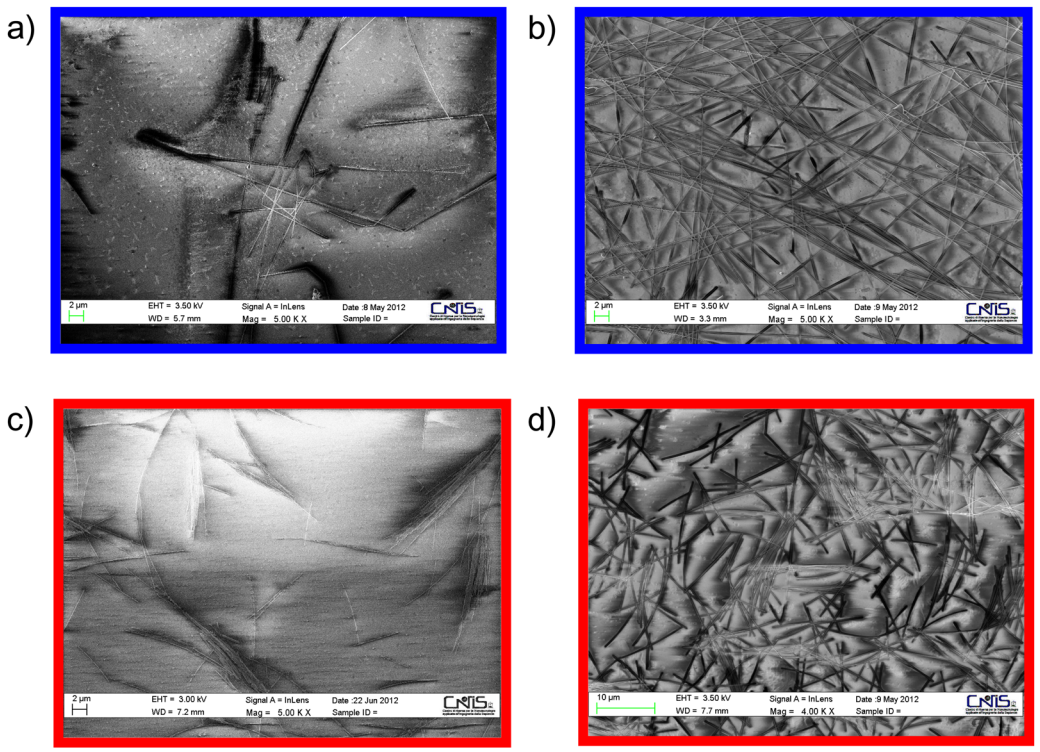

FIG. 2. Scanning electron micrographs of the four NW silver nanowires deposited onto glass substrate (see Table I): Blue frame holds for long type nanowires (a) low density and (b) high density; red frame holds for short type nanowires (c) low and (d) high density, respectively. Same magnification was employed for all samples.

analog display for setting of temperature of the integrated heater allows to set the temperature with a resolution of ~10 °C. However, once the hotplate temperature is set with this resolution, the actual temperature is accurately read by a thermocouple, which is placed in direct contact with the heating plate.

In order to avoid oscillation of the heating current, a stabilized power supply was employed. A radiometric forward looking infrared (FLIR) camera operating in the long wavelength infrared range was used to measure the amount of infrared radiation emitted by the four different samples between 8 and 12 μm, providing detailed thermographic images. The FPA sensor of this radiometric imaging system is based on a grid of 320 × 240 pixels, made of vanadium oxide (VOx) uncooled microbolometers, having a pixel size characteristic length of 25 μm (pitch) and a noise equivalent temperature difference (NETD) of 80 mK, usually referred as the sensitivity of the sensor. For preventing detector saturation, the temperature of sample holder was never set above 90 °C. A complete set of infrared images were recorded by placing the samples in direct contact with the heating holder and by acquiring consecutive images, during both heating and cooling processes, with a time step of 60 s. In this configuration, the wires' coatings are facing the infrared camera, in order to avoid sample deterioration. In the resulting infrared images, the four Ag-nanowires samples were observed in the meantime, while the image of the background heated surface was taken as a reference. In order to prevent thermal reflection on the sample surface generated by external environmental sources, the camera/sample setup was protected by black opaque shields, thus confining the complete camera field of view (FOV).

In Figure 3, we report an example of image taken with the radiometric camera. This image was recorded after the samples were taken for approximately 12 min at the fixed temperature of 60 °C. Looking at the corresponding colorbar, it can be recognized that the four samples, namely, NW1, NW2 NW3, and NW4, appear to be darker, with respect to the heating substrate, i.e., after being at the high temperature for 12 min, the infrared images of Ag nanowires films show only a weak bleaching. The different sample positions are evidenced with colored rectangles, while further details can be found within Figure 3 caption. It is worth to mention that an attempt was made in order to use the bare glass substrate as a reference but its infrared images were completely dissolved in the hotplate image, due to the high absorbance of glass in the 10 μm range.

The digital images were then analyzed with MATLAB software in order to retrieve the analytical values from the images data. For each sample, a uniform area was selected over the images and the data arising from the selected image's pixels were numerically integrated so to obtain the mean value of the resulting IR intensity level, which was then converted into temperature data by means of thermocouple output data. Given a set of consecutive images, the data collected are reported in Figure 4, where the resulting *apparent* temperature of NW samples as a function of time is given. During the first 25 min, the samples are slowly heated, then the current is switched off and the cooling behavior is also observed.

In particular, we observe that under the same heating conditions, of about 90 °C, the apparent temperature of the four nanowires samples qualitatively follows the trend of the corresponding heating holder temperature, i.e., the four curves have the same shape. This is no longer the case for their absolute values, being the apparent temperature of the four samples always below that of the driving heat source. Furthermore, there is a difference between the heating behaviour of low density samples NW1 and NW3, reaching the highest apparent temperature, and high density samples NW2 and NW4, whose apparent temperatures keep somewhat lower.

The obtained experimental results indicate that by keeping constant the wires' dimensions, IR signature effectiveness increases with increasing nanowires' density. At the same time, given a comparable metal filling factor, the short wires (i.e., NW3 and NW4) display a better shielding behaviour, with respect to the long wires (NW1 and NW2).

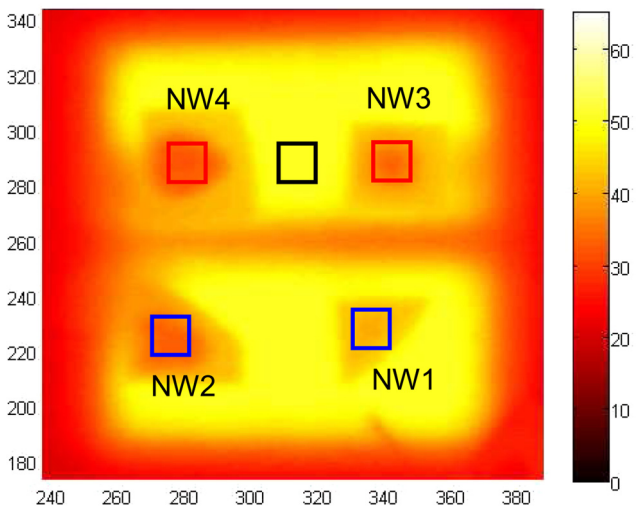

FIG. 3. Infrared image recorded with a long wavelength IR camera after 12 min of heating at about 60 °C. The four different samples, as well as the background heated surface taken as reference, are evidenced by the colored rectangles.

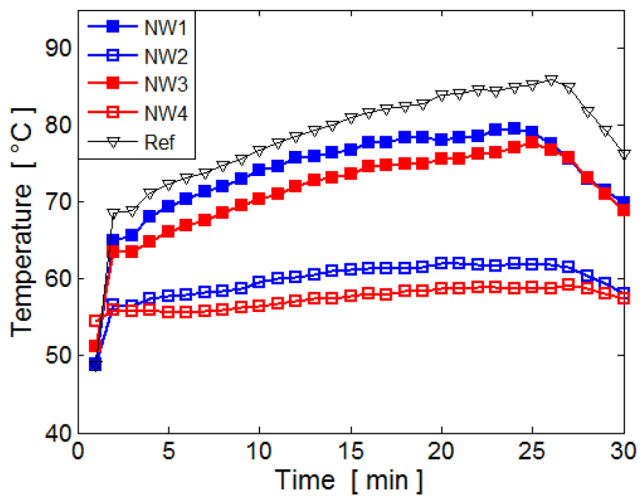

FIG. 4. Experimental plot of temperature evolution as a function of time, measured in the LWIR range, i.e., 8–12 μm, for the four different silver nanowires samples.

III. RESULTS AND DISCUSSIONS

In order to explain the different values of the experimental curves, let us consider a composite with silver nanowires randomly aligned in plane. The permittivity dyadic of such a medium reads as follows:

$$\bar{\bar{\varepsilon}} = \begin{pmatrix} \varepsilon_{xx} & 0 & 0 \\ 0 & \varepsilon_{yy} & 0 \\ 0 & 0 & \varepsilon_{zz} \end{pmatrix}. \quad (1)$$

We used the mixing formulas for randomly orientated ellipsoidal inclusions reported in Ref. 27, to calculate the relative permittivity of an effective medium

$$\varepsilon_{eff} = \varepsilon_e + \varepsilon_e \frac{\frac{f}{3}\sum_{j=x,y,z} \frac{\varepsilon_i - \varepsilon_e}{\varepsilon_e + N_j(\varepsilon_i - \varepsilon_e)}}{1 - \frac{f}{3}\sum_{j=x,y,z} \frac{N_j(\varepsilon_i - \varepsilon_e)}{\varepsilon_e + N_j(\varepsilon_i - \varepsilon_e)}}, \quad (2)$$

where ε_e and ε_i are the relative permittivities of the host matrix and the wires, respectively, f represents the metal filling factor, and N_j ($j = x, y, z$, $N_x + N_y + N_z = 1$) are the depolarisation factors.[27] Equation (2) was opportunely modified for metallic needles randomly aligned in the xy plane, i.e., within the film surface (see Figure 1). As a result, the following expressions are obtained for the transverse, $\varepsilon_{xx} = \varepsilon_{yy}$, and for the perpendicular ε_{zz} dyadic components:

$$\varepsilon_{xx} = \varepsilon_{yy} = \varepsilon_e + \frac{f}{2}\varepsilon_e(\varepsilon_i - \varepsilon_e)\frac{\frac{1}{\varepsilon_e} + \frac{1}{\varepsilon_e + (\varepsilon_i - \varepsilon_e)/2}}{1 - \frac{f}{4}\frac{(\varepsilon_i - \varepsilon_e)}{\varepsilon_e + (\varepsilon_i - \varepsilon_e)/2}} \quad (3)$$

and

$$\varepsilon_{zz} = \varepsilon_e + f(\varepsilon_i - \varepsilon_e). \quad (4)$$

Considering composites of air-surrounded nanowires, we assumed $\varepsilon_e = 1$, while the optical constants of silver were taken from Ref. 28. The metal filling factor f is also reported in Table I, being evaluated from SEM top-view images by means of their colour contrast.

Since the radiometric emission was detected at normal incidence, i.e., perpendicularly to films' surface, we assume that the radiation polarization is equally distributed along the xy plane. Following these considerations, the real and imaginary part of the permittivity components, $\varepsilon_{xx} = \varepsilon_{yy}$, were calculated for the four different silver nanowires meshes in the whole IR investigated range, as shown in Figure 5. According to Kirchoff's law of thermal radiation, there is a correspondence between thermal emissivity and absorption, thus the experimental results are interpreted via the corresponding absorbance spectra.[8] The refractive index and extinction coefficients were retrieved for the silver nanowires systems, being $\mathrm{Re}(\varepsilon) = n^2 - k^2$ and $\mathrm{Im}(\varepsilon) = 2nk$, and used to recover the spectral absorbance A from $A = 1 - |T| - |R|$, where the transmission coefficient T and the reflection coefficient R are obtained by applying the transfer matrix method.

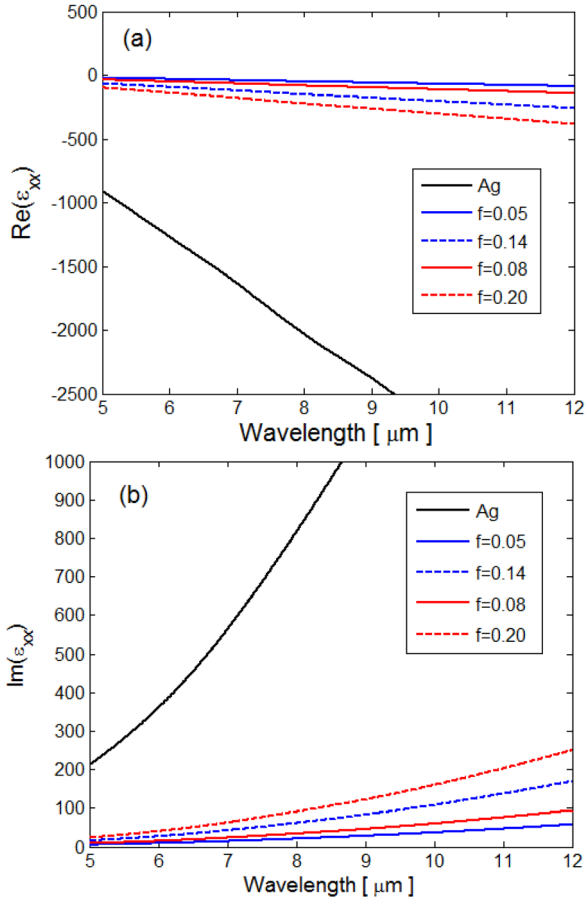

FIG. 5. Plot of the real (a) and imaginary (b) part of the relative effective permittivity components, $\varepsilon_{xx} = \varepsilon_{yy}$, calculated for the four nanowires' mesh whose filling factors are given in Table I. For comparison, the black curve corresponds to the permittivity of silver.[28]

In Figure 6, these results are summarized for the four different films, whose thickness is supposed to be proportional to wires' diameter, considering a SiO_2 substrate. It is notable that the combination of different thicknesses and filling factors may produce different absorbance dispersions, which in turns result in a different trend of the experimental curves.

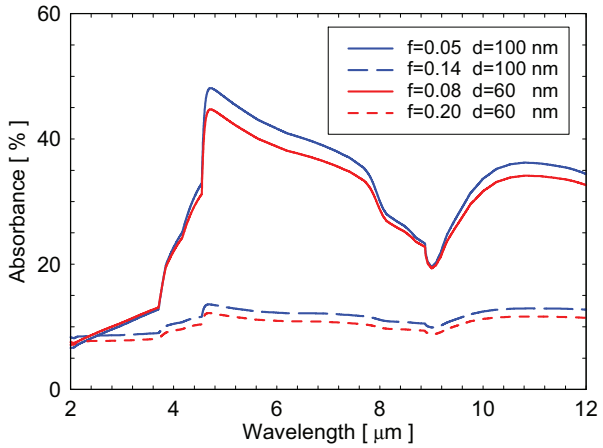

FIG. 6. Plot of the absorbance spectra evaluated from the refractive index and extinction coefficient, for the four nanowires' sample having different geometrical thicknesses, as reported in Table I. For all calculated curves, the substrate is SiO_2.

It is worth to observe that metals in general pertain very high reflectance values in the IR range, thus for a metal-based film, the higher the metal content, in terms of either thickness or filling factor, the lower the absorbance in the IR range. In other words, as the film metal content increases, its dielectric constant value becomes closer to that of silver, which behaves—in the IR—as a mirror. Given this statement, we notice that sample NW1 presents the highest absorbance values within the whole investigated wavelength range. Being sample NW1 thicker ($d = 100$ nm) than sample NW3 ($d = 60$ nm), its metal filling factor is supposed to be somewhat lower ($f = 0.05$) with respect to that of sample NW3 ($f = 0.08$). Same considerations hold for the two high density samples, resulting in the filling factor of sample NW3 which is lower ($f = 0.14$) than that of sample NW4 ($f = 0.20$).

Finally, from the reconstruction of the absorbance curves plotted in Figure 6, the influence of the substrate is evidenced by the oscillations, resembling SiO_2 absorption dispersion, particularly for low filling factor values. By using a substrate not strongly absorbing in the IR range, as for instance CaF_2, the absorbance curves of nanowires films would be smoothed and the absorption peak would disappear.

IV. CONCLUSIONS

In conclusion, we have performed an experimental investigation of different films composed of randomly oriented silver nanowires deposited onto glass substrate. In order to separate the contribution from two key parameters as wires' dimensions (both diameter and length) and metal filling factor, we prepared some nanowires' films using two different sized wires and two concentrations for the starting solutions. Infrared emission measurements under heating regime were performed in the wavelength range included between 8 and 12 μm, i.e., one of the two atmospheric windows pertaining high IR transmittance. Using a FPA infrared camera, as well as a thermocouple, we observed samples' temperature evolution under heating regime and we find that silver nanowires films display an apparent temperature always keeping below that of the driving heat source. The different experimental curves can be interpreted in terms of different absorbance spectra of films, derived from effective permittivity calculations, as a function of metal filling factor. For the investigated set of samples, experimental results indicate that the efficiency of IR signature reduction in the 8–12 μm range is improves with increasing filling factor.

As a conclusion, randomly oriented silver nanowires meshes allow to perform a thermal camouflage of the underlying heat source, giving an apparent temperature which can also be intentionally heterogeneous, i.e., by modifying wires concentration of the starting solution in order to prepare different areas with variable metal fraction. The easiness of sample preparation along with the possibility to control the filling factor value makes these structures promising candidate for absorbance, and thus emittance, tailoring. The obtained results are rather encouraging and pave the way to the design of infrared selective absorber/emitter, by opportunely choosing wires' geometrical parameters and concentration, as well as by opportunely selecting a surrounding medium other than air.

ACKNOWLEDGMENTS

This work has been performed in the framework of the project "FISEDA" granted by Italian Ministry of Defence. Professor Mario Bertolotti is kindly acknowledged for helpful discussion and interesting comments.

[1]N. Liu, M. Mesch, T. Weiss, M. Hentschel, and H. Giessen, "Infrared perfect absorber and its application as plasmonic sensor," Nano Lett. **10**, 2342 (2010).
[2]J. J. Greffet, R. Carminati, K. Joulain, J. P. Mulet, S. Mainguy, and Y. Chen, "Coherent emission of light by thermal sources," Nature **416**, 61 (2002).
[3]N. Mattiucci, G. D'Aguanno, A. Alù, C. Agryropoulos, J. V. Foreman, and M. J. Bloemer, "Taming the thermal emissivity of metals: A metamaterial approach," Appl. Phys. Lett. **100**, 201109 (2012).
[4]R. Li Voti, M. C. Larciprete, G. Leahu, C. Sibilia, and M. Bertolotti, "Optimization of thermochromic VO_2 based structures with tunable thermal emissivity," J. Appl. Phys. **112**, 034305 (2012).
[5]R. Li Voti, M. C. Larciprete, G. Leahu, C. Sibilia, and M. Bertolotti, "Optical response of multilayer thermochromic VO_2-based structures," J. Nanophotonics **6**, 061601 (2012).
[6]G. D'Aguanno, M. C. Larciprete, N. Mattiucci, A. Belardini, M. J. Bloemer, E. Fazio, O. Buganov, M. Centini, and C. Sibilia, "Experimental study of Bloch vector analysis in nonlinear, finite, dissipative systems," Phys. Rev. A **81**, 013834 (2010).
[7]S. Y. Lin, J. G. Fleming, D. L. Hetherington, B. K. Smith, R. Biswas, K. M. Ho, M. M. Sigalas, W. Zubrzycki, S. R. Kurtz, and J. Bur, "A three-dimensional photonic crystal operating at infrared wavelengths," Nature **394**, 251 (1998).
[8]R. Li Voti, Rom. Rep. Phys. **64**(2), 446–466 (2012).
[9]J. G. Fleming, S. Y. Lin, I. El-Kady, R. Biswas, and K. M. Ho, "All-metallic three-dimensional photonic crystals with a large infrared bandgap," Nature **417**, 52 (2002).
[10]P. J. Hesketh, J. N. Zemel, and B. Gebhart, "Organ pipe radiant modes of periodic micromachined silicon surfaces," Nature **324**, 549 (1986).
[11]J. T. K. Wan, "Tunable thermal emission at infrared frequencies via tungsten gratings," Opt. Commun. **282**, 1671 (2009).
[12]J. Hao, J. Wang, X. Liu, W. J. Padilla, L. Zhou, and M. Qiu, "High performance optical absorber based on a plasmonic metamaterial," Appl. Phys. Lett. **96**, 251104 (2010).
[13]J. A. Mason, S. Smith, and D. Wasserman, "Strong absorption and selective thermal emission from a midinfrared metamaterial," Appl. Phys. Lett. **98**, 241105 (2011).
[14]Y. Cui, J. Xu, K. H. Fung, Y. Jin, A. Kumar, S. He, and N. X. Fang, "A thin film broadband absorber based on multi-sized nanoantennas," Appl. Phys. Lett. **99**, 253101 (2011).
[15]S. P. Mahulikar, H. R. Sonawane, and G. Arvind Rao, "Infrared signature studies of aerospace vehicles," Prog. Aerosp. Sci. **43**, 218 (2007).
[16]Y. Sun, "Silver nanowires—Unique templates for functional nanostructures," Nanoscale **2**, 1626 (2010).
[17]J.-Q. Hu, Q. Chen, Z.-X. Xie, G.-B. Han, R.-H. Wang, B. Ren, Y. Zhang, Z.-L. Yang, and Z.-Q. Tian, "A simple and effective route for the synthesis of crystalline silver nanorods and nanowires," Adv. Funct. Mater. **14**, 183 (2004).
[18]A. Belardini, M. C. Larciprete, M. Centini, E. Fazio, C. Sibilia, D. Chiappe, C. Martella, A. Toma, M. Giordano, and F. Buatier de Mongeot, "Circular dichroism in the optical second-harmonic emission of curved gold metal nanowires," Phys. Rev. Lett. **107**, 257401 (2011).
[19]A. Belardini, M. C. Larciprete, M. Centini, E. Fazio, C. Sibilia, M. Bertolotti, A. Toma, D. Chiappe, and F. B. De Mongeot, "Tailored second harmonic generation from self-organized metal nano-wires arrays," Opt. Express **17**, 3603–3609 (2009).
[20]A. Belardini, F. Pannone, G. Leahu, M. C. Larciprete, M. Centini, C. Sibilia, C. Martella, M. Giordano, M. Giordano, D. Chiappe, and F. Buatier de Mongeot, "Evidence of anomalous refraction of self-assembled curved gold nanowires," Appl. Phys. Lett. **100**, 251109 (2012).

[21]D. R. Smith and D. Schurig, "Electromagnetic wave propagation in media with indefinite permittivity and permeability tensors," Phys. Rev. Lett. **90**, 077405 (2003).
[22]Y. Liu, G. Bartal, and X. Zhang, "All-angle negative refraction and imaging in a bulk medium made of metallic nanowires in the visible region," Opt. Express **16**, 15439 (2008).
[23]J. Yao, Z. Liu, Y. Liu, Y. Wang, C. Sun, G. Bartal, A. M. Stacy, and X. Zhang, "Optical negative refraction in bulk metamaterials of nanowires," Science **321**, 930 (2008).
[24]J. Y. Lee, S. T. Connor, Y. Cui, and P. Peumans, "Solution-processed metal nanowire mesh transparent electrodes," Nano Lett. **8**, 689 (2008).
[25]F. Toschi, S. Orlanducci, V. Guglielmotti, I. Cianchetta, C. Magni, M. L. Terranova, M. Pasquali, E. Tamburri, R. Matassa, and M. Rossi, "Hybrid C-nanotubes/Si 3D nanostructures by one-step growth in a dual-plasma reactor," Chem. Phys. Lett. **539–540**, 94–101 (2012).
[26]M. L. Terranova, D. Manno, M. Rossi, A. Serra, E. Filippo, S. Orlanducci, and E. Tamburri, "Self-assembly of N-diamond nanocrystals into supercrystals," Cryst. Growth Des. **9**, 1245–1249 (2009).
[27]A. Sihvola, *Electromagnetic Mixing Formulas and Applications* (The Institution of Electrical Engineers, London, UK, 1999).
[28]"Handbook of optical constants of solids," *Subpart 1: Metals*, edited by Edward D. Palik (Academic Press, 1985).